



# From $\kappa$ to $\chi$ : Evaluating Hygroscopicity-Based Mixing State Estimates with a Particle-Resolved Model

Yicen Liu<sup>a</sup>, Jian Wang<sup>b</sup>, and Nicole Riemer<sup>c</sup>

<sup>a</sup>Department of Civil and Environmental Engineering, Grainger College of Engineering, University of Illinois Urbana-Champaign, Urbana, IL, USA

<sup>b</sup>Department of Energy, Environmental, and Chemical Engineering, Washington University in St. Louis, St. Louis, MO, USA

<sup>c</sup>Department of Climate, Meteorology, and Atmospheric Science, University of Illinois Urbana-Champaign, Urbana, IL, USA

**Correspondence:** Nicole Riemer (nriemer@illinois.edu)

**Abstract.** Aerosol mixing state strongly influences how particles interact with clouds, radiation, and atmospheric chemistry, but it remains difficult to quantify from routine observations. The aerosol mixing state index ( $\chi$ ) typically requires detailed single-particle composition data, available only from particle-resolved models or advanced measurements. Yuan and Zhao (2023) proposed estimating  $\chi$  from in-situ hygroscopicity ( $\kappa$ ) measurements using a hygroscopicity tandem differential mobility analyzer (HTDMA), offering a promising observational pathway. However, their method assumes a binary system of more- and less-hygroscopic components, which may not represent aerosol populations containing intermediate-hygroscopicity species. Here, we systematically evaluate this  $\kappa$ -based  $\chi$  retrieval using the stochastic particle-resolved model PartMC-MOSAIC. We generated a large ensemble of aerosol populations from urban plume simulations spanning a wide range of emissions, aging conditions, and meteorology. For each population and particle diameter (50–250 nm), we compared the “true” mixing state index from per-particle composition ( $\chi^{\text{PMC}}$ ) with the  $\chi$  inferred from  $\kappa$  distributions ( $\chi^{\text{YZ}}$ ). The retrieval performs well for many aerosol populations, but systematically overestimates  $\chi$  when externally mixed intermediate-hygroscopicity components violate the binary assumption. By quantifying the error distributions across particle sizes, we derive uncertainty bounds for the retrieval and apply them to long-term HTDMA datasets from urban, continental, and coastal sites, providing a first multi-site assessment of seasonal variability in  $\chi$  inferred from hygroscopicity measurements.

## 15 1 Introduction

Atmospheric aerosols are complex mixtures of different chemical species. The chemical composition of aerosols governs their role in key atmospheric processes, including the ability to act as cloud condensation nuclei (CCN) (Hallberg et al., 1994; Leck et al., 2002; Cubison et al., 2008; Leck and Svensson, 2015), interactions with incoming solar radiation (Patterson, 1981; Ravishankara et al., 2015; Drame et al., 2015), and capacity to facilitate heterogeneous reactions (George and Abbatt, 2010; H. Bertram et al., 2018; Baustian et al., 2012). These processes depend not only on the bulk chemical composition but also on how different chemical species are distributed among and within individual particles, a characteristic termed the aerosol mixing state (Riemer and West, 2013). Aerosol populations can be “internally mixed”, where all particles possess the same composition as the bulk, or “externally mixed”, where each particle consists of a single chemical species. However, field



measurements reveal that real atmospheric aerosols fall between these two extremes, exhibiting complex mixing states that  
25 evolve through processes such as coagulation, condensation, chemical aging, and transport (Laskin et al., 2002; Ebert et al.,  
2004; Kleinman et al., 2008; Li et al., 2010; Sun et al., 2013; Adachi et al., 2022; Yoo et al., 2024).

To quantify the degree of internal versus external mixing, Riemer and West (2013) proposed the aerosol mixing state index  
( $\chi$ ), which applies information-theoretic (Shannon) entropy to the distribution of chemical species among particles based on  
per-particle mass fractions. For any aerosol population,  $\chi$  ranges from 0% (fully external mixture) to 100% (fully internal  
30 mixture). The metric has been applied to evaluate the mixing state assumptions for air quality modeling (Zhu et al., 2016),  
examine the evolution of particle mixing structure (Li et al., 2016), and assess mixing state heterogeneity impacts on black  
carbon light absorption enhancement (Zeng et al., 2024). Direct calculation of  $\chi$  requires detailed single-particle composition  
data, which can be obtained through either single-particle measurement techniques or particle-resolved models.

While several studies have successfully computed  $\chi$  using single-particle techniques such as aerosol time-of-flight mass  
35 spectrometry (ATOFMS), computer-controlled scanning electron microscopy/energy dispersive X-ray spectroscopy (CCSEM/EDX),  
Scanning Transmission X-ray Microscopy/Near Edge Fine Structure spectroscopy (STXM/NEXAFS) (Wu et al., 2024; O'Brien  
et al., 2015; Fraund et al., 2017; Bondy et al., 2018; Lata et al., 2021; Singh et al., 2021; M. Tomlin et al., 2022; Cheng et al.,  
2023; Xue et al., 2024a; Sharpe et al., 2025; Rivera-Adorno et al., 2025), and single-particle soot photometer (SP2) (Yu  
et al., 2020; Zhao et al., 2021a), they remain relatively rare and campaign-specific. Similarly, particle-resolved models such as  
40 PartMC-MOSAIC (Particle Monte Carlo-Model for Simulating Aerosol Interactions and Chemistry) have been used to com-  
pute  $\chi$  and investigate mixing state evolution (Shou et al., 2019; Gasparik et al., 2020; Zheng et al., 2021; Yao et al., 2022;  
Jiang et al., 2025; Zhang et al., 2025), but are computationally intensive and cannot be applied directly to observational datasets  
without extensive additional information. These limitations motivate a shift toward approaches that infer  $\chi$  from more routinely  
available aerosol measurements.

45 Hygroscopicity measurements offer a promising way to infer aerosol mixing state. Aerosol hygroscopicity describes the  
ability of particles to take up water, and its dependence on chemical composition is characterized by the hygroscopicity param-  
eter ( $\kappa$ ) (Petters and Kreidenweis, 2007). The  $\kappa$  value can be obtained from the hygroscopic growth factors using a hygroscopic  
Tandem Differential Mobility Analyzer (HTDMA) (Rader and McMurry, 1986) under subsaturated conditions, and are widely  
deployed at monitoring networks and field campaigns (Mochida et al., 2010; Adam et al., 2012; Yeung et al., 2014; Zhang  
50 et al., 2017; Phillips et al., 2018; Wang and Chen, 2019; Tao et al., 2023; Deshmukh et al., 2025). Importantly, HTDMA  
measurements yield not only mean  $\kappa$  values but also probability distributions of  $\kappa$  ( $\kappa$ -PDFs), which capture particle-to-particle  
heterogeneity in aerosol hygroscopicity while bypassing the need for single-particle composition data.

Accordingly, Yuan and Zhao (2023) proposed an elegant method (hereafter referred to as YZ) to infer  $\chi$  from HTDMA-  
measured  $\kappa$ -PDFs. In brief, YZ assumes that aerosols are binary mixtures of more-hygroscopic (MH) and less-hygroscopic  
55 (LH) components with distinct  $\kappa$  values, such that the measured  $\kappa$ -PDF can be mapped to the distribution of MH/LH volume  
fractions, from which  $\chi$  is computed. A key limitation is that the binary assumption may be violated in real atmospheric  
populations, as many aerosols may contain intermediate-hygroscopicity components, (e.g., secondary organic aerosol, SOA)



that do not fit neatly into either MH or LH categories. This oversimplification of chemical variability may introduce systematic biases in  $\chi$  estimates.

60 While the YZ method offers a practical approach, its performance under realistic atmospheric conditions remains poorly understood, particularly when particles contain substantial fractions of intermediate-hygroscopicity material. It is therefore unclear how large the bias in inferred  $\chi$  might be, under what conditions the method remains reliable, and when it begins to break down. These knowledge gaps raise questions about whether  $\chi$  derived from  $\kappa$ -PDFs can be applied confidently to long-term field datasets.

65 In this work, we evaluate the YZ method with particle-resolved simulations across diverse atmospheric conditions and particle sizes, quantifying both its accuracy and systematic biases associated with the assumption made to derive  $\chi$ . By benchmarking the YZ method against particle-resolved simulations, we identify the regimes in which  $\kappa$ -derived  $\chi$  can be interpreted with confidence, as well as conditions under which the underlying binary hygroscopicity assumption introduces systematic bias. We then apply the YZ method to long-term HTDMA measurements from four campaigns within the U.S. Department of  
70 Energy's Atmospheric Radiation Measurement (ARM) program. This study establishes the systematic evaluation of  $\chi$  derived from  $\kappa$ -only measurements and quantifies uncertainty ranges for  $\kappa$ -based mixing state retrievals, providing foundations for climatological applications.

The paper is structured as follows: Section 2 revisits the YZ algorithm, and Section 3 describes the particle-resolved model, validation scenario library, and HTDMA datasets. Section 4 examines the relationship between true  $\chi$  from per-particle com-  
75 position and estimated  $\chi$  using the YZ  $\kappa$ -based method. Section 5 presents  $\kappa$ -based  $\chi$  retrievals in field measurements.

## 2 Hygroscopicity-Based Aerosol Mixing State Metric ( $\chi$ )

The YZ method assumes each aerosol particle in the population consists of one or both of MH and LH components, with  $\kappa$  calculated as the volume-weighted average of  $\kappa_{\text{LH}}$  and  $\kappa_{\text{MH}}$ . For the aerosol with a given dry diameter and a known  $\kappa$ -PDF with  $X$  bins, the volume fractions of the LH ( $P_{i,\text{LH}}$ ) and MH ( $P_{i,\text{MH}}$ ) components at bin  $i$  ( $i = 1, 2, 3, \dots, X$ ) can be calculated  
80 as:

$$P_{i,\text{MH}} = \frac{\kappa_i - \kappa_{\text{LH}}}{\kappa_{\text{MH}} - \kappa_{\text{LH}}}, \quad (1)$$

$$P_{i,\text{LH}} = 1 - P_{i,\text{MH}}, \quad (2)$$

where  $\kappa_i$  is the  $\kappa$  at bin  $i$ .

85 The original YZ method used  $\kappa_{\text{LH}} = 0.01$  and  $\kappa_{\text{MH}} = 0.6$ . In our simulations, we expanded these bounds to  $\kappa_{\text{LH}} = 0$  (for nearly hydrophobic components such as BC) and  $\kappa_{\text{MH}} = 0.65$  (for highly hygroscopic inorganic species such as  $\text{SO}_4$ ,  $\text{NO}_3$ , and  $\text{NH}_4$ ). Expanding the bounds ensures that we capture the full spectrum of particle hygroscopicity simulated in PartMC. For future applications, these bounds can be flexibly chosen based on measured  $\kappa$  distributions from HTDMA, so that the binary system captures the observed range of hygroscopicities in the ambient aerosol population.



90 Particles selected by the HTDMA at a given dry diameter exhibit a finite size distribution determined by the DMA transfer function (Brechtel and Kreidenweis, 2000; Collins et al., 2004). The YZ method neglects this residual size dispersion and assumes that particles assigned to the same  $\kappa$ -bin are effectively monodisperse within instrumental resolution. Under this approximation, they are treated as having identical physicochemical properties and mixing entropy. The entropies can be obtained from the normalized  $\kappa$ -PDF:

$$95 \quad H_i = -P_{i,LH} \times \ln P_{i,LH} - P_{i,MH} \times \ln P_{i,MH}, \quad (3)$$

$$H_\alpha = \sum_{i=1}^X H_i \times c(\kappa)_i \times \Delta\kappa, \quad (4)$$

$$H_\gamma = -P_{LH} \times \ln P_{LH} - P_{MH} \times \ln P_{MH}, \quad (5)$$

100 where  $c(\kappa)_i$  is the probability density value of the normalized  $\kappa$ -PDF at bin  $i$ , and  $\Delta\kappa$  is the bin width,  $P_{LH}$  and  $P_{MH}$  are the respective volume fraction of the LH and MH components in the population, and they can be calculated by:

$$P_{LH} = \sum_{i=1}^X P_{i,LH} \times c(\kappa)_i \times \Delta\kappa \quad (6)$$

and

$$P_{MH} = \sum_{i=1}^X P_{i,MH} \times c(\kappa)_i \times \Delta\kappa \quad (7)$$

105 The species diversities are calculated from the mixing entropies as:

$$D_i = e^{H_i}, \quad (8)$$

$$D_\alpha = e^{H_\alpha}, \quad (9)$$

and

$$110 \quad D_\gamma = e^{H_\gamma}, \quad (10)$$

with  $D_i$ ,  $D_\alpha$ , and  $D_\gamma$  denote the diversity of the particle subpopulation represented by the  $i^{\text{th}}$   $\kappa$ -bin, average per-bin diversity, and bulk population diversity, respectively.

The hygroscopicity-based aerosol mixing state index  $\chi$  can be calculated as:

$$\chi = \frac{D_\alpha - 1}{D_\gamma - 1}, \quad (11)$$

115 which varies from 0% that all particles in the population purely consist of the LH or MH component to 100% that the LH and MH components are homogeneously distributed across all particles in the population with identical volume fractions.



### 3 Ensemble of Particle-Resolved Model Scenarios

#### 3.1 PartMC-MOSAIC Model Description

PartMC (Particle-resolved Monte Carlo) (Riemer et al., 2009) is a stochastic, zero-dimensional aerosol model that simulates the evolution of per-particle composition of an aerosol population within a well-mixed computational volume. The particle positions within the computational volume are not tracked. The composition of individual particles evolves through emission, dilution, and coagulation, modeled using a stochastic Monte Carlo approach. Dry and wet deposition of aerosol particles are not included.

To allow for the treatment of aerosol chemistry, PartMC is coupled to the aerosol chemistry model MOSAIC (Model for Simulating Aerosol Interactions and Chemistry) (Zaveri et al., 2008). This includes the gas phase photochemical mechanism CBM-Z (Carbon-Bond Mechanism) (Zaveri and Peters, 1999), the Multicomponent Taylor Expansion Method (MTEM) for estimating activity coefficients of electrolytes and ions in inorganic multicomponent solutions (Zaveri et al., 2005b), the Multicomponent Equilibrium Solver for Aerosols (MESA) to compute intraparticle solid-liquid partitioning (Zaveri et al., 2005a) and a solver for dynamic gas-particle partitioning (Zaveri et al., 2008). To simulate secondary organic aerosol (SOA) we use the SORGAM scheme (Schell et al., 2001). The CBM-Z gas phase mechanism includes 77 gaseous species. MOSAIC treats key aerosol species including sulfate ( $\text{SO}_4$ ), nitrate ( $\text{NO}_3$ ), ammonium ( $\text{NH}_4$ ), chloride (Cl), carbonate ( $\text{CO}_3$ ), methanesulfonic acid (MSA), sodium (Na), calcium (Ca), other inorganic mass (OIN), black carbon (BC), primary and secondary organic aerosol (POA and SOA). Species such as Cl, Na, Ca, and other mineral components are not included in this study. The simulations were conducted using PartMC version 2.6.1 and MOSAIC version 2019-01-05.

#### 3.2 Synthetic Validation scenario library

The details of the scenario library were described in Liu et al. (2025). In short, the scenario library generated from previous work focuses on urban environments, and in particular on the aging process of carbonaceous aerosol by coagulation and condensation of secondary aerosols, which result in changes in per-particle chemical composition. The simulations were performed in a two-stage process: a spin-up run starting from zero aerosol initial conditions, followed by a second run using randomly selected aerosol populations from the spin-up as initial conditions. Each 48-h simulation featured a diurnal emission pattern starting at 6 AM LST (local solar time), with aerosol and gas phase emissions during the 12 h daytime period, representing a well-mixed, polluted boundary layer. Then we discontinued emissions during the 12 h nighttime period, representing the polluted air remaining in the nocturnal residual layer. We repeated the same process 100 times using different input parameters, yielding 4,900 aerosol populations with diverse mixing states and chemical compositions. The input parameter space was constructed using a Latin hypercube sampling approach following the strategy of Zheng et al. (2021).

In this study, we used “ $\text{N}_2\text{O}_5$ -ON” as a synthetic validation library, though  $\text{N}_2\text{O}_5$  chemistry is not the focus of the current analysis. Note that primary sea salt emissions were not included in the library. Accordingly, the validation results presented here are primarily applicable to continental anthropogenic aerosol regimes. For each population, we first selected particles with dry diameter ( $D_p$ ) within narrow size ranges centered at 50, 100, 150, 200, and 250 nm (Table 1). This procedure mimics



**Table 1.** Diameter ranges replicate quasi-monodisperse particle selection in HTDMA measurements.

$D_p$ (nm)	$D_{p,\min}$ (nm)	$D_{p,\max}$ (nm)
50	47.3	52.6
100	94.2	105.6
150	140.7	159.1
200	186.8	212.9
250	232.7	267.1

150 HTDMA measurements, in which dry, quasi-monodisperse aerosol particles are selected using a differential mobility analyzer (DMA). We then calculated  $\chi$  using two approaches. First, we calculated  $\chi^{\text{PMC}}$  following the rigorous mixing-state framework of Riemer and West (2013), using single-particle volume fractions from the PartMC-MOSAIC output, which represents the true mixing state of each population. For the  $\chi^{\text{PMC}}$  calculation, species were assigned to low- or high-hygroscopic groups. The low-hygroscopic group comprised SOA species (ARO1, ARO2, ALK1, OLE1, API1, API2, LIM1, LIM2), OIN, OC, 155 and BC, while the high-hygroscopic group included  $\text{SO}_4$ ,  $\text{NO}_3$ , Cl,  $\text{NH}_4$ , MSA,  $\text{CO}_3$ , Na, and Ca. We then constructed the population-level  $\kappa$ -PDF based on individual particle hygroscopicity parameters  $\kappa$  derived from particle composition using the ZSR mixing rule, and applied the YZ method to obtain  $\chi^{\text{YZ}}$ . The deviation between  $\chi^{\text{PMC}}$  and  $\chi^{\text{YZ}}$  quantifies the systematic bias associated with the YZ method.

#### 4 Evaluation and interpretation of $\kappa$ -based mixing state indices

160 In this section, we first quantify the agreement between  $\kappa$ -based and particle-resolved mixing state indices across particle sizes, then examine the physical origin of systematic biases, and finally illustrate the non-uniqueness of bulk hygroscopicity metrics with respect to aerosol mixing state.

##### 4.1 Quantitative comparison of mixing state indices

Figure 1 compares the hygroscopicity-based aerosol mixing state indices estimated from the YZ method ( $\chi^{\text{YZ}}$ ) with those 165 computed from single-particle composition data ( $\chi^{\text{PMC}}$ ) for five dry diameters (50–250 nm) in the validation scenario library. The value of  $\chi^{\text{PMC}}$  represents the "true" mixing state by preserving the chemical composition and hygroscopicity of individual particles. Overall, the YZ method agrees well with the particle-resolved calculations, with a mean absolute error (MAE) of  $\sim 2\%$  across all diameters. However, notable overestimations are observed, particularly at 150 nm for more externally mixed populations ( $\chi^{\text{PMC}} < 40\%$ ), where the maximum bias ( $\Delta\chi = \chi^{\text{YZ}} - \chi^{\text{PMC}}$ ) reaches 29%. It is also worth noting that larger 170 errors are associated with SOA-rich populations. To investigate how the presence of intermediate-hygroscopicity components (e.g., SOA) breaks down the binary assumption, we next examine the  $\kappa$ -PDFs.

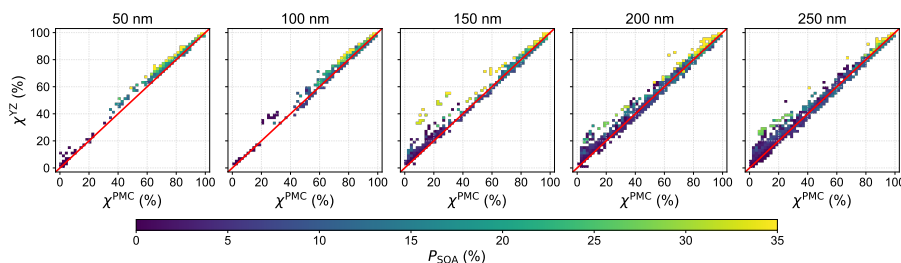


**Figure 1.** Scatter plots between  $\chi^{YZ}$  ( $\kappa$ -based mixing state estimates using the YZ method) and  $\chi^{PMC}$  (mixing state index computed from per-particle composition) for aerosols with dry diameters of 50, 100, 150, 200, 250 nm. Each point represents a particle population from the validation scenario library, with colors indicating the bulk SOA volume fraction. The red line shows the 1:1 relationship.

## 4.2 Systematic bias associated with intermediate-hygroscopicity components

For populations with higher SOA content, the bias in  $\chi$  depends critically on how the majority of SOA is mixed with other components (Figure 2). A large overestimation of  $\chi$  occurs when species are segregated into particles (Figure 2a), since a substantial fraction of pure SOA particles that do not fit into either the LH or MH categories introduce the bias. In contrast, when SOA is primarily internally mixed with hygroscopic species (Figure 2b), the bias becomes negligible.

To illustrate the fundamental limitation of the binary assumption in the YZ method, we constructed two simplified cases. First, consider a fully externally mixed population (Figure 2c) with half the particles pure SOA ( $\kappa_{SOA} = 0.1$ ) and half pure ammonium sulfate (AS;  $\kappa_{AS} = 0.65$ ). Under the binary assumption, the YZ method misinterprets pure SOA particles as artificial mixtures containing 15% MH species and 85% LH species. By assigning SOA particles a higher effective number of species than they physically contain, the method estimates a higher average per-particle diversity ( $D_\alpha$ ), thereby shifting the population toward a more internally mixed state. Alternatively, consider a monodispersed population (Figure 2d) in which each particle is an internal mixture of 50% SOA and 50% AS. In this case, all particles have the same  $\kappa$  of 0.375, resulting in a narrow, unimodal  $\kappa$ -PDF. The YZ method correctly identifies this state ( $\chi^{YZ} = 1$ ), as the bulk population diversity directly reflects the average per-particle diversity ( $D_\gamma = D_\alpha$ ).

These examples demonstrate that systematic overestimation of  $\chi$  arises specifically when intermediate-hygroscopicity components are externally mixed, causing the  $\kappa$ -based binary mapping to misclassify chemically simple particles as artificial mixtures.

## 4.3 Constructing confidence intervals for $\chi$ retrievals

We quantified the uncertainty associated with  $\kappa$ -based mixing state retrievals by computing the retrieval errors ( $\Delta\chi = \chi^{YZ} - \chi^{PMC}$ ) from Figure 1 and summarizing its distribution in Figure 3. The retrieval exhibits a systematic positive bias across all particle sizes and the uncertainty (width of the shaded area) increases with diameter. Notably, the error remains within

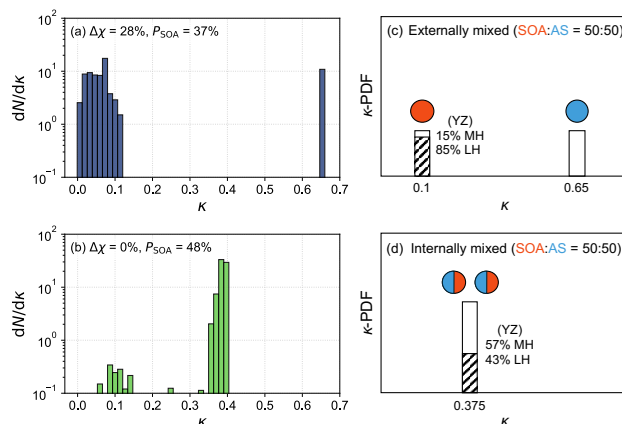


**Figure 2.** (a and b) The  $\kappa$ -PDFs of two high-SOA (secondary organic aerosol) content aerosol populations at a dry diameter of 150 nm from the validation scenario library. Note that y-axes are in logarithmic scale. (c and d) Schematic diagrams of simplified cases with identical bulk compositions of 50% SOA and 50% ammonium sulfate (AS).

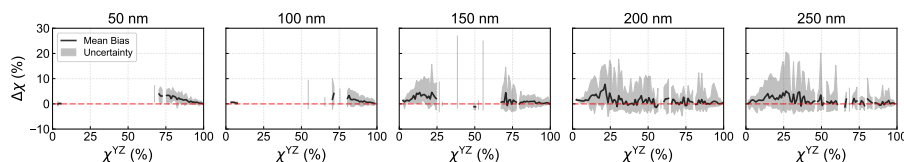


**Figure 3.** Error distribution of  $\chi$  retrieval from Figure 1. Solid lines represent the mean bias and shaded areas show the uncertainty range (2.5<sup>th</sup>–97.5<sup>th</sup> percentiles of the error). Gaps correspond to  $\chi$  ranges with insufficient particle samples to estimate statistics.

$\pm 10\%$  for  $\chi > 70\%$  for all diameters, indicating a reliable retrieval regime for more internally mixed populations. These error distributions are subsequently applied to quantify uncertainties in  $\chi$  retrieved from long-term HTDMA measurements.

#### 195 4.4 Non-uniqueness of bulk hygroscopicity with respect to mixing state

Before turning to field applications, we use the particle-resolved simulations to illustrate a more general property of aerosol populations: bulk hygroscopicity alone does not uniquely determine aerosol mixing state. Figure 4 illustrates how aerosol mixing state is encoded in particle-to-particle variability rather than bulk hygroscopicity alone. From the full scenario library, we identified seven populations with a dry diameter of 150 nm that share the same mean hygroscopicity ( $\kappa_{\text{mean}}=0.31$ ) but differ 200 markedly in their particle-level composition distributions and mixing state indices. This example highlights that even within a narrow size range, particles can exhibit substantial variability in composition, a defining characteristic of aerosol mixing state that the particle-resolved model explicitly resolves.

Because  $\kappa_{\text{mean}}$  constrains only the bulk fraction of less- and more-hygroscopic material, these populations are indistinguishable based on  $\kappa_{\text{mean}}$  alone. In more externally mixed populations, ( $\chi^{\text{pmc}} < 30\%$ ), the distribution of  $P_{\text{MH}}$  is dominated

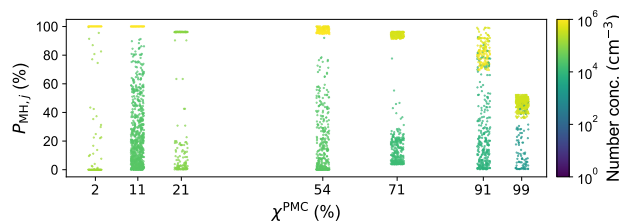


**Figure 4.** Strip plot of more-hygroscopic (MH) component volume fractions ( $P_{\text{MH},j}$ ) for particles at  $D_p = 150$  nm. The seven aerosol populations shown have identical mean hygroscopicity ( $\kappa_{\text{mean}} = 0.31$ ) but different mixing state indices ( $\chi^{\text{PMC}}$ ). Colors indicate number concentration.

205 by two distinct modes near 0 and 100%, indicating segregation of hygroscopic components among particles. As the populations become increasingly internally mixed ( $\chi^{\text{PMC}} \rightarrow 1$ ), these modes broaden and merge, and the distribution of  $P_{\text{MH}}$  becomes continuous and centered at intermediate values. For nearly fully internally mixed populations, the distinction between subpopulations is effectively lost.

This result is consistent with the conceptual analysis of Yuan and Zhao (2023), and we explicitly demonstrate through  
 210 particle-resolved simulations that identical mean hygroscopicity can correspond to fundamentally different aerosol mixing states. Information on particle-to-particle variability, as quantified by the mixing state index  $\chi$ , is therefore required to distinguish aerosol populations with the same  $\kappa_{\text{mean}}$ .

## 5 Mixing state retrievals from long-term HTDMA measurements

Having quantified the performance and limitations of  $\kappa$ -based mixing state retrievals using particle-resolved simulations, we  
 215 now apply the method to long-term hygroscopicity measurements to examine aerosol mixing state in real atmospheric environments.

### 5.1 Typical $\kappa$ distributions in field measurements

An example of HTDMA-measured  $\kappa$ -PDFs across the four ARM sites is shown in Figure 5, which can be considered as the normalized aerosol number fractions varied with  $\kappa$  between 0 and 0.65. These long-term averaged  $\kappa$ -PDFs are often broad  
 220 and, in some cases, distinctly multi-modal, indicating substantial particle-to-particle hygroscopicity heterogeneity. Notably, the distributions for 50 nm particles consistently peak at lower  $\kappa$  values and exhibit narrower spreads compared to larger particles across all sites, likely reflecting the greater abundance of freshly emitted, low-hygroscopicity combustion particles.

While the shape and structure of these  $\kappa$ -PDFs provide insight into aerosol mixing state, they do not uniquely determine chemical composition. A given  $\kappa$  value may arise from different combinations of chemical species, and without additional  
 225 speciation measurements, one cannot reliably attribute a peak in the distribution to a particular aerosol type of chemical

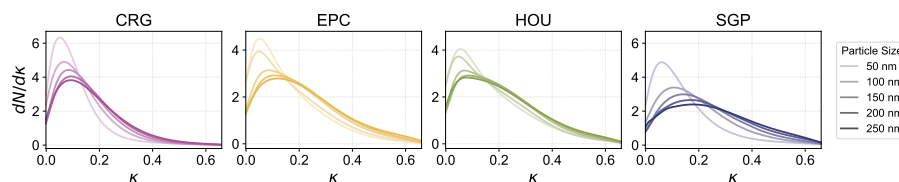


**Figure 5.** Campaign-averaged  $\kappa$ -PDFs for 50, 100, 150, 200, and 250 nm particles. Each panel represents a different site from the U.S. Department of Energy (DOE) Atmospheric Radiation Measurement (ARM) program: Baltimore, MD (CRG); La Jolla, CA (EPC); Houston, TX (HOU); Southern Great Plains, OK (SGP). Particle sizes are distinguished by opacity, with larger particles shown as more opaque.

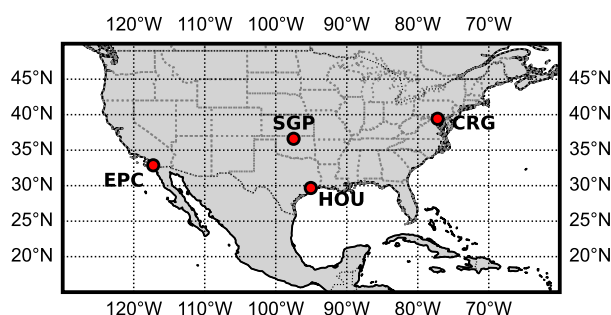


**Figure 6.** Map of ARM sites with long-term HTDMA measurements: Baltimore, MD (CRG); La Jolla, CA (EPC); Houston, TX (HOU); and Southern Great Plains, OK (SGP).

component. Therefore, mapping from hygroscopicity distributions to aerosol mixing state is non-trivial and needs careful consideration when making compositional assumptions.

## 5.2 Long-term $\chi$ retrievals from ARM measurements

In this section, we apply the YZ method to multi-year HTDMA datasets (2021–2025) from four U.S. Department of Energy Atmospheric Radiation Measurement (DOE ARM) campaigns (Uin et al., 2012): CoURAGE (CRG), TRACER (HOU), Southern Great Plains (SGP), and ECAPE (EPC). Figure 6 shows the geographical location of the sites. For each HTDMA dataset, we extracted  $\kappa$  and particle number concentrations at specified dry diameters to construct  $\kappa$ -PDFs, which were then applied in the YZ framework to calculate  $\chi^{YZ}$ .

The time series of  $\chi^{YZ}$  is shown in Figure 7. Across all sites and seasons,  $\chi^{YZ}$  typically falls between 70% and 90%, a regime where our model evaluation indicates that the  $\kappa$ -based retrieval is generally reliable. Comparable ranges have been reported in Chengdu measurements (60%–90%) using the same method (Yuan and Zhao, 2023). This prevalence of intermediate-to-high  $\chi$  values is consistent with previous studies suggesting predominantly internally mixed aerosol populations (Zhao et al., 2021b; Xue et al., 2024b), although definitions of  $\chi$  vary among studies (i.e., not necessarily based on LH/MH species). Temporal variability remains modest, with  $\chi^{YZ}$  varying within  $\pm 10\%$  across the observational period, suggesting that atmospheric aging



240 and mixing processes consistently maintain high degrees of internal mixing despite variations in meteorological conditions  
and source influences, consistent with previously reported rapid daytime soot aging and mixing (Riemer et al., 2004; Wang  
et al., 2010). The HOU site shows generally lower  $\chi^{YZ}$  values compared to other continental sites, reflecting the influence of  
diverse local emission sources in the Houston metropolitan area that have insufficient time for atmospheric aging. Farley et al.  
(2024) reported a broader range of  $\chi$  (5%–95%) at this site due to differences in the definition of  $\chi$  from this study. However,  
245 the overall trend toward a more externally mixed particle population at HOU remains consistent. During winter, large particles  
at the coastal site (EPC) exhibit lower  $\chi^{YZ}$  values than the continental sites, indicating a stronger influence of marine and  
transported aerosols that remain partially externally mixed.

### 5.3 Limitations of the YZ method

Particle-resolved simulations demonstrate that the YZ method provides a statistically robust framework for inferring aerosol  
250 mixing state under a wide range of conditions, and field applications show that the approach can be applied consistently to  
observational datasets. The approach performs reliably across various atmospheric regimes, but systematically overestimates  
 $\chi$  when the population is SOA-rich and intermediate-hygroscopicity components are externally mixed. Incorporation of uncer-  
tainty estimates derived from particle-resolved modeling enables the inferred relationships to be applied rigorously to long-term  
observational datasets.

255 While our synthetic library does not include marine aerosol populations, the binary hygroscopicity framework can be con-  
ceptually extended to such environments. In marine-influenced environments where sea salt constitutes a major fraction of  
the aerosol population, the hygroscopicity spectrum extends beyond that of typical continental inorganic species, requiring  
the inclusion of highly hygroscopic particles with  $\kappa$  approaching the value for sea salt ( $\kappa \approx 1.28$ ). To assess the implication  
of shifting the  $\kappa$ -based end-member values, we repeated the analysis in Section 4.2 using  $\kappa_{MH} = 1.28$ . The results indicate a  
260 substantial overestimation of  $\chi$ , with the largest biases observed in externally mixed populations, reaching up to 86%. Note  
that the validation library contains no pure sea-salt particles, therefore this analysis does not represent a realistic marine case.  
Instead, it serves to establish an upper bound on the retrieval error arising from a mismatch between  $\kappa_{MH}$  end-member and the  
“true” inorganic hygroscopicity of the population.

The sensitivity to end-member choice can be understood by examining how the binary framework reinterprets particle com-  
265 position. In the original binary representation with  $\kappa_{MH} = 0.65$ , the MH end-member corresponds to inorganic salts typical  
of continental environments (sulfate, nitrate, ammonium). However, this assumption becomes inconsistent in the presence of  
sea salt ( $\kappa \approx 1.28$ ) particles. In a marine-influenced environment, prescribing  $\kappa_{MH} = 1.28$  effectively redefines the MH end-  
member as pure sea salt. As a result, a particle of  $\kappa = 0.65$  becomes compositionally ambiguous. Such a particle may represent  
either an internally mixed organic sea-salt particle or a pure non-marine inorganic particle. In the first scenario, the particle is  
270 correctly interpreted as a mixture of LH and MH components. In the second scenario, however, the binary framework misclas-  
sifies a pure non-marine inorganic particle as internally mixed, introducing structural uncertainty and artificially increasing the  
inferred degree of internal mixing.

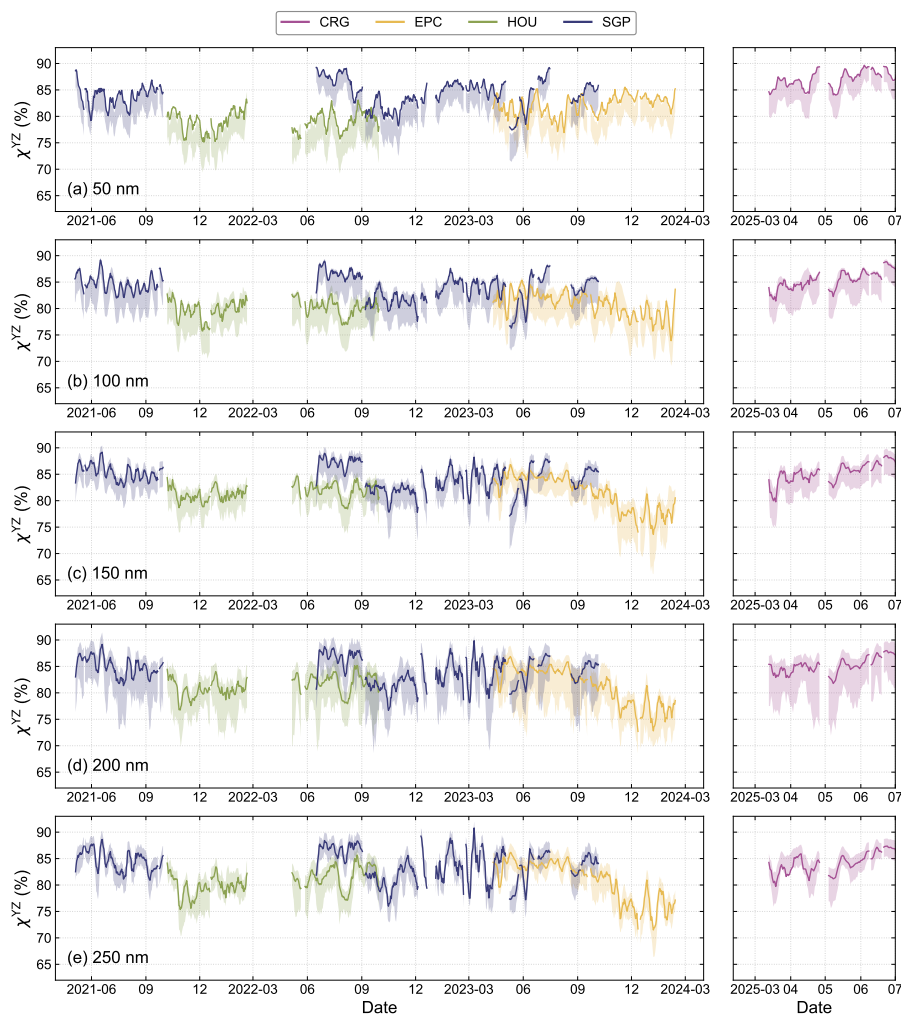


**Figure 7.** Time series of  $\chi^{YZ}$  for particles with dry diameters of (a) 50 nm, (b) 100 nm, (c) 150 nm, (d) 200 nm, and (e) 250 nm at four Atmospheric Radiation Measurement (ARM) program sites. Lines represent 7-day moving averages, and shaded areas indicate the 95% range of uncertainty.

The coexistence of multiple inorganic species with substantially different  $\kappa$  values limits the ability of particle hygroscopicity to retrieve the aerosol mixing state. More generally,  $\kappa$ -based end-member values are only constrained by observations when particles close to the pure-component hygroscopicity are present; when hygroscopic components are systematically internally mixed, end-members may be latent in the  $\kappa$ -PDF, rendering  $\chi$  retrievals sensitive to assumed bounds rather than directly observable quantities.

Despite these limitations, the method remains broadly applicable across a wide range of continental and mixed aerosol environments where hygroscopicity distributions are sufficiently constrained and aerosol populations are not strongly externally



280 mixed with respect to intermediate-hygroscopicity components. In such cases, including many environments where SOA is present but largely internally mixed,  $\kappa$ -based  $\chi$  retrievals provide a robust characterization of aerosol mixing state. Its strength lies in enabling statistically consistent inference from long-term observational datasets, particularly in regions characterized by more internally mixed populations.

## 6 Conclusions

285 This study presents a comprehensive evaluation of the hygroscopicity-based aerosol mixing state index ( $\chi$ ) derived from HTDMA measurements using the method proposed by Yuan and Zhao (2023). By enabling aerosol mixing state metrics to be inferred from routinely available hygroscopicity measurements, the approach of Yuan and Zhao (2023) provides an important practical pathway for extending the mixing state analyses to long-term observational datasets. Using a large ensemble of particle-resolved (PartMC–MOSAIC) simulations, we quantify the performance and systematic limitations of inferring  $\chi$  from  
290  $\kappa$  distributions under realistic atmospheric conditions.

Overall, the YZ method agrees well with PartMC-MOSAIC simulations across a wide range of particle sizes and mixing states (MAE~2%). Systematic overestimation of  $\chi$  arises when intermediate-hygroscopicity components, such as secondary organic aerosol, are predominantly externally mixed, violating the binary hygroscopicity assumption that underlies the retrieval. In most atmospheric scenarios, however, including cases where SOA is present but largely internally mixed, the method pro-  
295 vides a robust approximation of aerosol mixing state from long-term hygroscopicity measurements, enabling systematic analysis of field datasets where detailed composition information is unavailable. Application to ambient measurements reveals that  $\kappa$ -derived  $\chi$  values typically range from 70% to 90%, indicating a high degree of internal mixing in observed aerosol populations.

Similarly, the presence of highly hygroscopic species that exceed the upper bound of the assumed binary spectrum (e.g.,  
300 sea salt with  $\kappa>1$ ) requires calibration of the hygroscopicity thresholds, which constrains the hygroscopicity separation among aerosol types and degrades retrieval accuracy. These limitations should be considered when applying the YZ method to aerosol populations dominated by externally mixed intermediate- or highly-hygroscopic species.

*Code availability.* PartMC v2.6.1 is archived at <https://zenodo.org/records/5644422>.

<https://doi.org/10.5194/egusphere-2026-1724>

Preprint. Discussion started: 2 April 2026

© Author(s) 2026. CC BY 4.0 License.



305 *Author contributions.* YL conducted the data analysis and drafted the manuscript. JW provided guidance on the interpretation of HTDMA measurements and reviewed the manuscript. NR supervised the research and contributed to the study design. All authors contributed to the discussion of the results.

*Competing interests.* The authors declare that they have no conflict of interest.

*Acknowledgements.* This work was supported by DOE ASR grant DE-SC0025197.



## References

- 310 Adachi, K., Tobo, Y., Koike, M., Freitas, G., Zieger, P., and Krejci, R.: Composition and Mixing State of Arctic Aerosol and Cloud Residual Particles from Long-Term Single-Particle Observations at Zeppelin Observatory, Svalbard, *Atmospheric Chemistry and Physics*, 22, 14 421–14 439, <https://doi.org/10.5194/acp-22-14421-2022>, 2022.
- Adam, M., Putaud, J. P., Martins dos Santos, S., Dell’Acqua, A., and Gruening, C.: Aerosol Hygroscopicity at a Regional Background Site (Ispra) in Northern Italy, *Atmospheric Chemistry and Physics*, 12, 5703–5717, <https://doi.org/10.5194/acp-12-5703-2012>, 2012.
- 315 Baustian, K. J., Cziczo, D. J., Wise, M. E., Pratt, K. A., Kulkarni, G., Hallar, A. G., and Tolbert, M. A.: Importance of Aerosol Composition, Mixing State, and Morphology for Heterogeneous Ice Nucleation: A Combined Field and Laboratory Approach, *Journal of Geophysical Research: Atmospheres*, 117, <https://doi.org/10.1029/2011JD016784>, 2012.
- Bondy, A. L., Bonanno, D., Moffet, R. C., Wang, B., Laskin, A., and Ault, A. P.: The Diverse Chemical Mixing State of Aerosol Particles in the Southeastern United States, *Atmospheric Chemistry and Physics*, 18, 12 595–12 612, <https://doi.org/10.5194/acp-18-12595-2018>,  
320 2018.
- Brechtel, F. J. and Kreidenweis, S. M.: Predicting Particle Critical Supersaturation from Hygroscopic Growth Measurements in the Humidified TDMA. Part I: Theory and Sensitivity Studies, *Journal of the Atmospheric Sciences*, 57, 1854–1871, [https://doi.org/10.1175/1520-0469\(2000\)057<1854:PPCSFH>2.0.CO;2](https://doi.org/10.1175/1520-0469(2000)057<1854:PPCSFH>2.0.CO;2), 2000.
- Cheng, Z., Morgenstern, M., Henning, S., Zhang, B., Roberts, G. C., Fraund, M., Marcus, M. A., Lata, N. N., Fialho, P., Mazzoleni, L., Wehner, B., Mazzoleni, C., and China, S.: Cloud Condensation Nuclei Activity of Internally Mixed Particle Populations at a Remote Marine Free Troposphere Site in the North Atlantic Ocean, *Science of The Total Environment*, 904, 166 865, <https://doi.org/10.1016/j.scitotenv.2023.166865>, 2023.
- 325 Collins, D. R., Cocker, D. R., Flagan, R. C., and Seinfeld, J. H.: The Scanning DMA Transfer Function, *Aerosol Science and Technology*, 38, 833–850, <https://doi.org/10.1080/027868290503082>, 2004.
- 330 Cubison, M. J., Ervens, B., Feingold, G., Docherty, K. S., Ulbrich, I. M., Shields, L., Prather, K., Hering, S., and Jimenez, J. L.: The Influence of Chemical Composition and Mixing State of Los Angeles Urban Aerosol on CCN Number and Cloud Properties, *Atmospheric Chemistry and Physics*, 8, 5649–5667, <https://doi.org/10.5194/acp-8-5649-2008>, 2008.
- Deshmukh, S., Poulain, L., Wehner, B., Henning, S., Petit, J.-E., Fombelle, P., Favez, O., Herrmann, H., and Pöhlker, M.: External Particle Mixing Influences Hygroscopicity in a Sub-Urban Area, *Atmospheric Chemistry and Physics*, 25, 741–758, <https://doi.org/10.5194/acp-25-741-2025>, 2025.
- 335 Drame, M. S., Ceamanos, X., Roujean, J. L., Boone, A., Lafore, J. P., Carrer, D., and Geoffroy, O.: On the Importance of Aerosol Composition for Estimating Incoming Solar Radiation: Focus on the Western African Stations of Dakar and Niamey during the Dry Season, *Atmosphere*, 6, 1608–1632, <https://doi.org/10.3390/atmos6111608>, 2015.
- Ebert, M., Weinbruch, S., Hoffmann, P., and Ortner, H. M.: The Chemical Composition and Complex Refractive Index of Rural and Urban Influenced Aerosols Determined by Individual Particle Analysis, *Atmospheric Environment*, 38, 6531–6545, <https://doi.org/10.1016/j.atmosenv.2004.08.048>, 2004.
- 340 Farley, R. N., Lee, J. E., Rivellini, L.-H., Lee, A. K. Y., Dal Porto, R., Cappa, C. D., Gorkowski, K., Shawon, A. S. M., Benedict, K. B., Aiken, A. C., Dubey, M. K., and Zhang, Q.: Chemical Properties and Single-Particle Mixing State of Soot Aerosol in Houston during the TRACER Campaign, *Atmospheric Chemistry and Physics*, 24, 3953–3971, <https://doi.org/10.5194/acp-24-3953-2024>, 2024.



- 345 Fraund, M., Pham, D. Q., Bonanno, D., Harder, T. H., Wang, B., Brito, J., De Sá, S. S., Carbone, S., China, S., Artaxo, P., Martin, S. T., Pöhlker, C., Andreae, M. O., Laskin, A., Gilles, M. K., and Moffet, R. C.: Elemental Mixing State of Aerosol Particles Collected in Central Amazonia during GoAmazon2014/15, *Atmosphere*, 8, 173, <https://doi.org/10.3390/atmos8090173>, 2017.
- Gasparik, J. T., Ye, Q., Curtis, J. H., Presto, A. A., Donahue, N. M., Sullivan, R. C., West, M., and Riemer, N.: Quantifying Errors in the Aerosol Mixing-State Index Based on Limited Particle Sample Size, *Aerosol Science and Technology*, 54, 1527–1541, <https://doi.org/10.1080/02786826.2020.1804523>, 2020.
- 350 George, I. J. and Abbatt, J. P. D.: Heterogeneous Oxidation of Atmospheric Aerosol Particles by Gas-Phase Radicals, *Nature Chemistry*, 2, 713–722, <https://doi.org/10.1038/nchem.806>, 2010.
- H. Bertram, T., E. Cochran, R., H. Grassian, V., and A. Stone, E.: Sea Spray Aerosol Chemical Composition: Elemental and Molecular Mimics for Laboratory Studies of Heterogeneous and Multiphase Reactions, *Chemical Society Reviews*, 47, 2374–2400, <https://doi.org/10.1039/C7CS00008A>, 2018.
- 355 Hallberg, A., Ogren, J. A., Noone, K. J., Okada, K., Heintzenberg, J., and Svenningsson, I. B.: The Influence of Aerosol Particle Composition on Cloud Droplet Formation, *Journal of Atmospheric Chemistry*, 19, 153–171, <https://doi.org/10.1007/BF00696587>, 1994.
- Jiang, F., Zheng, Z., Coe, H., Healy, R. M., Poulain, L., Gros, V., Zhang, H., Li, W., Liu, D., West, M., Topping, D., and Riemer, N.: Integrating Simulations and Observations: A Foundation Model for Estimating the Aerosol Mixing State Index, *ACS ES&T Air*, 2, 877–890, <https://doi.org/10.1021/acsestair.4c00329>, 2025.
- 360 Kleinman, L. I., Springston, S. R., Daum, P. H., Lee, Y.-N., Nunnermacker, L. J., Senum, G. I., Wang, J., Weinstein-Lloyd, J., Alexander, M. L., Hubbe, J., Ortega, J., Canagaratna, M. R., and Jayne, J.: The Time Evolution of Aerosol Composition over the Mexico City Plateau, *Atmospheric Chemistry and Physics*, 8, 1559–1575, <https://doi.org/10.5194/acp-8-1559-2008>, 2008.
- Laskin, A., Iedema, M. J., and Cowin, J. P.: Quantitative Time-Resolved Monitoring of Nitrate Formation in Sea Salt Particles Using a CCSEM/EDX Single Particle Analysis, *Environmental Science & Technology*, 36, 4948–4955, <https://doi.org/10.1021/es020551k>, 2002.
- 365 Lata, N. N., Zhang, B., Schum, S., Mazzoleni, L., Brimberry, R., Marcus, M. A., Cantrell, W. H., Fialho, P., Mazzoleni, C., and China, S.: Aerosol Composition, Mixing State, and Phase State of Free Tropospheric Particles and Their Role in Ice Cloud Formation, *ACS Earth and Space Chemistry*, 5, 3499–3510, <https://doi.org/10.1021/acsearthspacechem.1c00315>, 2021.
- Leck, C. and Svensson, E.: Importance of Aerosol Composition and Mixing State for Cloud Droplet Activation over the Arctic Pack Ice in Summer, *Atmospheric Chemistry and Physics*, 15, 2545–2568, <https://doi.org/10.5194/acp-15-2545-2015>, 2015.
- 370 Leck, C., Norman, M., Bigg, E. K., and Hillamo, R.: Chemical Composition and Sources of the High Arctic Aerosol Relevant for Cloud Formation, *Journal of Geophysical Research: Atmospheres*, 107, AAC 1–1–AAC 1–17, <https://doi.org/10.1029/2001JD001463>, 2002.
- Li, W., Shao, L., Wang, Z., Shen, R., Yang, S., and Tang, U.: Size, Composition, and Mixing State of Individual Aerosol Particles in a South China Coastal City, *Journal of Environmental Sciences*, 22, 561–569, [https://doi.org/10.1016/S1001-0742\(09\)60146-7](https://doi.org/10.1016/S1001-0742(09)60146-7), 2010.
- 375 Li, W., Sun, J., Xu, L., Shi, Z., Riemer, N., Sun, Y., Fu, P., Zhang, J., Lin, Y., Wang, X., Shao, L., Chen, J., Zhang, X., Wang, Z., and Wang, W.: A Conceptual Framework for Mixing Structures in Individual Aerosol Particles, *Journal of Geophysical Research: Atmospheres*, 121, 13,784–13,798, <https://doi.org/10.1002/2016JD025252>, 2016.
- Liu, Y., Yao, Y., Curtis, J. H., West, M., and Riemer, N.: The Impacts of Aerosol Mixing State on Heterogeneous N<sub>2</sub>O<sub>5</sub> Hydrolysis, *Aerosol Science and Technology*, 59, 402–423, <https://doi.org/10.1080/02786826.2024.2443587>, 2025.
- 380 M. Tomlin, J., Weis, J., P. Veghte, D., China, S., Fraund, M., He, Q., Reicher, N., Li, C., A. Jankowski, K., A. Rivera-Adorno, F., C. Morales, A., Rudich, Y., C. Moffet, R., K. Gilles, M., and Laskin, A.: Chemical Composition and Morphological Analysis of Atmospheric Particles



- from an Intensive Bonfire Burning Festival, *Environmental Science: Atmospheres*, 2, 616–633, <https://doi.org/10.1039/D2EA00037G>, 2022.
- 385 Mochida, M., Nishita-Hara, C., Kitamori, Y., Aggarwal, S. G., Kawamura, K., Miura, K., and Takami, A.: Size-Segregated Measurements of Cloud Condensation Nucleus Activity and Hygroscopic Growth for Aerosols at Cape Hedo, Japan, in Spring 2008, *Journal of Geophysical Research: Atmospheres*, 115, <https://doi.org/10.1029/2009JD013216>, 2010.
- O'Brien, R. E., Wang, B., Laskin, A., Riemer, N., West, M., Zhang, Q., Sun, Y., Yu, X.-Y., Alpert, P., Knopf, D. A., Gilles, M. K., and Moffet, R. C.: Chemical Imaging of Ambient Aerosol Particles: Observational Constraints on Mixing State Parameterization, *Journal of Geophysical Research: Atmospheres*, 120, 9591–9605, <https://doi.org/10.1002/2015JD023480>, 2015.
- 390 Patterson, E. M.: Optical Properties of the Crustal Aerosol: Relation to Chemical and Physical Characteristics, *Journal of Geophysical Research: Oceans*, 86, 3236–3246, <https://doi.org/10.1029/JC086iC04p03236>, 1981.
- Petters, M. D. and Kreidenweis, S. M.: A Single Parameter Representation of Hygroscopic Growth and Cloud Condensation Nucleus Activity, *Atmospheric Chemistry and Physics*, 7, 1961–1971, <https://doi.org/10.5194/acp-7-1961-2007>, 2007.
- Phillips, B. N., Royalty, T. M., Dawson, K. W., Reed, R., Petters, M. D., and Meskhidze, N.: Hygroscopicity- and Size-Resolved Measurements of Submicron Aerosol on the East Coast of the United States, *Journal of Geophysical Research: Atmospheres*, 123, 1826–1839, <https://doi.org/10.1002/2017JD027702>, 2018.
- 395 Rader, D. J. and McMurry, P. H.: Application of the Tandem Differential Mobility Analyzer to Studies of Droplet Growth or Evaporation, *Journal of Aerosol Science*, 17, 771–787, [https://doi.org/10.1016/0021-8502\(86\)90031-5](https://doi.org/10.1016/0021-8502(86)90031-5), 1986.
- Ravishankara, A. R., Rudich, Y., and Wuebbles, D. J.: Physical Chemistry of Climate Metrics, *Chemical Reviews*, 115, 3682–3703, <https://doi.org/10.1021/acs.chemrev.5b00010>, 2015.
- 400 Riemer, N. and West, M.: Quantifying Aerosol Mixing State with Entropy and Diversity Measures, *Atmospheric Chemistry and Physics*, 13, 11 423–11 439, <https://doi.org/10.5194/acp-13-11423-2013>, 2013.
- Riemer, N., Vogel, H., and Vogel, B.: Soot Aging Time Scales in Polluted Regions during Day and Night, *Atmospheric Chemistry and Physics*, 4, 1885–1893, <https://doi.org/10.5194/acp-4-1885-2004>, 2004.
- 405 Riemer, N., West, M., Zaveri, R. A., and Easter, R. C.: Simulating the Evolution of Soot Mixing State with a Particle-resolved Aerosol Model, *Journal of Geophysical Research*, 114, D09 202, <https://doi.org/10.1029/2008JD011073>, 2009.
- Rivera-Adorno, F. A., Tomlin, J. M., Lata, N. N., Azzarello, L., Robinson, M. A., Washenfelder, R. A., Franchin, A., Middlebrook, A. M., China, S., Brown, S. S., Young, C. J., Fraund, M., Moffet, R. C., and Laskin, A.: Chemical Imaging of Atmospheric Biomass Burning Particles from North American Wildfires, *ACS ES&T Air*, 2, 508–521, <https://doi.org/10.1021/acsestair.4c00242>, 2025.
- 410 Schell, B., Ackermann, I. J., Hass, H., Binkowski, F. S., and Ebel, A.: Modeling the Formation of Secondary Organic Aerosol within a Comprehensive Air Quality Model System, *Journal of Geophysical Research: Atmospheres*, 106, 28 275–28 293, <https://doi.org/10.1029/2001JD000384>, 2001.
- Sharpe, S., Li, Y., Benjemia, S., Rivera-Adorno, F., Olayemi, T., Ese, J., Shen, X., Fraund, M., Moffet, R., Nahar Lata, N., Cheng, Z., China, S., R. Homeyer, C., Dykema, J., A. Marcus, M., Wang, J., Cziczo, D., Keutsch, F., and Laskin, A.: Chemical Imaging of Individual Stratospheric Particles Sampled over North America, *Environmental Science: Atmospheres*, <https://doi.org/10.1039/D5EA00127G>, 2025.
- 415 Shou, C., Riemer, N., Onasch, T. B., Sedlacek, A. J., Lambe, A. T., Lewis, E. R., Davidovits, P., and West, M.: Mixing State Evolution of Agglomerating Particles in an Aerosol Chamber: Comparison of Measurements and Particle-Resolved Simulations, *Aerosol Science and Technology*, 53, 1229–1243, <https://doi.org/10.1080/02786826.2019.1661959>, 2019.



- Singh, N., Banerjee, T., Deboudt, K., Chakraborty, A., Khan, M. F., and Latif, M. T.: Sources, Composition, and Mixing State of Submicron Particulates over the Central Indo-Gangetic Plain, *ACS Earth and Space Chemistry*, 5, 2052–2065, <https://doi.org/10.1021/acsearthspacechem.1c00130>, 2021.
- Sun, Y., Wang, Z., Fu, P., Jiang, Q., Yang, T., Li, J., and Ge, X.: The Impact of Relative Humidity on Aerosol Composition and Evolution Processes during Wintertime in Beijing, China, *Atmospheric Environment*, 77, 927–934, <https://doi.org/10.1016/j.atmosenv.2013.06.019>, 2013.
- 425 Tao, J., Kuang, Y., Luo, B., Liu, L., Xu, H., Ma, N., Liu, P., Xue, B., Zhai, M., Xu, W., Xu, W., and Sun, Y.: Kinetic Limitations Affect Cloud Condensation Nuclei Activity Measurements Under Low Supersaturation, *Geophysical Research Letters*, 50, e2022GL101603, <https://doi.org/10.1029/2022GL101603>, 2023.
- Uin, J., Cromwell, E., Hayes, C., and Salwen, C.: Atmospheric Radiation Measurement (ARM) User Facility. Humidified Tandem Differential Mobility Analyzer (AOSHTDMA), updated daily. 2025-03-13 to 2025-11-30, ARM Mobile Facility (CRG), Baltimore, MD: Supplemental Facility 2 in rural setting (S2); 2023-02-15 to 2024-02-13, ARM Mobile Facility (EPC), La Jolla, CA: AMF1 (main site for ECAPE on Scripps Pier) (M1); 2021-10-01 to 2022-09-30, ARM Mobile Facility (HOU), Houston, TX: AMF1 (main site for TRACER) (M1); 2021-04-27 to 2023-10-24, Southern Great Plains (SGP), Lamont, OK (Extended and Co-located with C1) (E13). Compiled by Uin, J., Cromwell, E., Hayes, C., and Salwen, C. Data set accessed 2025-08-06 at <https://doi.org/10.5439/1776643>, 2012.
- 430 Wang, J., Cubison, M. J., Aiken, A. C., Jimenez, J. L., and Collins, D. R.: The Importance of Aerosol Mixing State and Size-Resolved Composition on CCN Concentration and the Variation of the Importance with Atmospheric Aging of Aerosols, *Atmospheric Chemistry and Physics*, 10, 7267–7283, <https://doi.org/10.5194/acp-10-7267-2010>, 2010.
- Wang, Y. and Chen, Y.: Significant Climate Impact of Highly Hygroscopic Atmospheric Aerosols in Delhi, India, *Geophysical Research Letters*, 46, 5535–5545, <https://doi.org/10.1029/2019GL082339>, 2019.
- 440 Wu, J., Liu, J., Gunsch, M. J., Mirrielees, J. A., Moffett, C. E., Zhang, Q., Sheesley, R. J., and Pratt, K. A.: Quantifying the Diversity of an Atmospheric Aerosol Population in an Arctic Oil Field on a Single-Particle Level, *Journal of Geophysical Research: Atmospheres*, 129, e2024JD041001, <https://doi.org/10.1029/2024JD041001>, 2024.
- Xue, J., Zhang, T., Park, K., Yan, J., Yoon, Y. J., Park, J., and Wang, B.: Diverse Sources and Aging Change the Mixing State and Ice Nucleation Properties of Aerosol Particles over the Western Pacific and Southern Ocean, *Atmospheric Chemistry and Physics*, 24, 7731–7754, <https://doi.org/10.5194/acp-24-7731-2024>, 2024a.
- 445 Xue, J., Zhang, T., Park, K., Yan, J., Yoon, Y. J., Park, J., and Wang, B.: Diverse Sources and Aging Change the Mixing State and Ice Nucleation Properties of Aerosol Particles over the Western Pacific and Southern Ocean, *Atmospheric Chemistry and Physics*, 24, 7731–7754, <https://doi.org/10.5194/acp-24-7731-2024>, 2024b.
- Yao, Y., Curtis, J. H., Ching, J., Zheng, Z., and Riemer, N.: Quantifying the Effects of Mixing State on Aerosol Optical Properties, *Atmospheric Chemistry and Physics*, 22, 9265–9282, <https://doi.org/10.5194/acp-22-9265-2022>, 2022.
- 450 Yeung, M. C., Lee, B. P., Li, Y. J., and Chan, C. K.: Simultaneous HTDMA and HR-ToF-AMS Measurements at the HKUST Supersite in Hong Kong in 2011, *Journal of Geophysical Research: Atmospheres*, 119, 9864–9883, <https://doi.org/10.1002/2013JD021146>, 2014.
- Yoo, H., Wu, L., Geng, H., and Ro, C.-U.: Physicochemical and Temporal Characteristics of Individual Atmospheric Aerosol Particles in Urban Seoul during KORUS-AQ Campaign: Insights from Single-Particle Analysis, *Atmospheric Chemistry and Physics*, 24, 853–867, <https://doi.org/10.5194/acp-24-853-2024>, 2024.



- 455 Yu, C., Liu, D., Broda, K., Joshi, R., Olfert, J., Sun, Y., Fu, P., Coe, H., and Allan, J. D.: Characterising Mass-Resolved Mixing State of Black Carbon in Beijing Using a Morphology-Independent Measurement Method, *Atmospheric Chemistry and Physics*, 20, 3645–3661, <https://doi.org/10.5194/acp-20-3645-2020>, 2020.
- Yuan, L. and Zhao, C.: Quantifying Particle-to-Particle Heterogeneity in Aerosol Hygroscopicity, *Atmospheric Chemistry and Physics*, 23, 3195–3205, <https://doi.org/10.5194/acp-23-3195-2023>, 2023.
- 460 Zaveri, R. A. and Peters, L. K.: A New Lumped Structure Photochemical Mechanism for Large-Scale Applications, *Journal of Geophysical Research: Atmospheres*, 104, 30 387–30 415, <https://doi.org/10.1029/1999JD900876>, 1999.
- Zaveri, R. A., Easter, R. C., and Peters, L. K.: A Computationally Efficient Multicomponent Equilibrium Solver for Aerosols (MESA), *Journal of Geophysical Research: Atmospheres*, 110, <https://doi.org/10.1029/2004JD005618>, 2005a.
- Zaveri, R. A., Easter, R. C., and Wexler, A. S.: A New Method for Multicomponent Activity Coefficients of Electrolytes in Aqueous Atmospheric Aerosols, *Journal of Geophysical Research: Atmospheres*, 110, <https://doi.org/10.1029/2004JD004681>, 2005b.
- 465 Zaveri, R. A., Easter, R. C., Fast, J. D., and Peters, L. K.: Model for Simulating Aerosol Interactions and Chemistry (MOSAIC), *Journal of Geophysical Research: Atmospheres*, 113, <https://doi.org/10.1029/2007JD008782>, 2008.
- Zeng, L., Tan, T., Zhao, G., Du, Z., Hu, S., Shang, D., and Hu, M.: Overestimation of Black Carbon Light Absorption Due to Mixing State Heterogeneity, *npj Climate and Atmospheric Science*, 7, 2, <https://doi.org/10.1038/s41612-023-00535-8>, 2024.
- 470 Zhang, F., Wang, Y., Peng, J., Ren, J., Collins, D., Zhang, R., Sun, Y., Yang, X., and Li, Z.: Uncertainty in Predicting CCN Activity of Aged and Primary Aerosols, *Journal of Geophysical Research: Atmospheres*, 122, 11,723–11,736, <https://doi.org/10.1002/2017JD027058>, 2017.
- Zhang, Z., Wang, J., Wang, J., Riemer, N., Liu, C., Jin, Y., Tian, Z., Cai, J., Cheng, Y., Chen, G., Wang, B., Wang, S., and Ding, A.: Steady-State Mixing State of Black Carbon Aerosols from a Particle-Resolved Model, *Atmospheric Chemistry and Physics*, 25, 1869–1881, <https://doi.org/10.5194/acp-25-1869-2025>, 2025.
- 475 Zhao, G., Tan, T., Zhu, Y., Hu, M., and Zhao, C.: Method to Quantify Black Carbon Aerosol Light Absorption Enhancement with a Mixing State Index, *Atmospheric Chemistry and Physics*, 21, 18 055–18 063, <https://doi.org/10.5194/acp-21-18055-2021>, 2021a.
- Zhao, G., Tan, T., Zhu, Y., Hu, M., and Zhao, C.: Method to Quantify Black Carbon Aerosol Light Absorption Enhancement with a Mixing State Index, *Atmospheric Chemistry and Physics*, 21, 18 055–18 063, <https://doi.org/10.5194/acp-21-18055-2021>, 2021b.
- Zheng, Z., West, M., Zhao, L., Ma, P.-L., Liu, X., and Riemer, N.: Quantifying the Structural Uncertainty of the Aerosol Mixing State Representation in a Modal Model, *Atmospheric Chemistry and Physics*, 21, 17 727–17 741, <https://doi.org/10.5194/acp-21-17727-2021>, 2021.
- 480 Zhu, S., Sartelet, K. N., Healy, R. M., and Wenger, J. C.: Simulation of Particle Diversity and Mixing State over Greater Paris: A Model–Measurement Inter-Comparison, *Faraday Discussions*, 189, 547–566, <https://doi.org/10.1039/C5FD00175G>, 2016.